STUDY OF SHEAR RATES IN SPINNING PROCESS OF KAOLIN/POLYETHERSULFONE (PESf) MEMBRANE PRECURSOR: EFFECT ON FIBER MORPHOLOGY

Mohd Suffian Misaran, Rosalam Sarbatly and Md. Mizanur Rahman
Faculty of Engineering, Universiti Malaysia Sabah, Kota Kinabalu, Sabah, Malaysia
E-Mail: suffian@ums.edu.my

ABSTRACT

The influence of shear stress induced by spinneret geometry on morphology of Kaolin/PESf hollow fiber membranes has been studied. Different extrusion rates at two different rheology properties were introduced on a straight spinneret resulting in various shear rates. The hollow fiber membrane were spun using the wet spinning method to decouple the effect of shear and elongation stress due to gravity stretched drawing and bore fluid rate factors. The morphology of the spun hollow fiber was observed under Scanning Electron Microscope (SEM). Shear rates at the tip of the spinneret annulus were calculated and visualize using a computational fluid dynamics model. Simulation data shows that extrusion rate increment increases the shear rate at the spinneret wall while fluid velocity maximize at the centre of annulus. The maximum shear rate recorded was 431 s^{-1} at an extrusion pressure of 0.5 bar. It is observed that higher shear rates increases the density of the finger like voids and ultimately affect the hollow fiber performance in general.

Keywords: shear flow, non-newtonian, spinnerets, hollow fiber, morphology.

INTRODUCTION

Membrane technologies have expanded extensively since the first asymmetric cellulose membrane was developed [1]. It plays an important role in water treatment, gas separation and environmental works. It comes in various structures such as the flat sheet, spiral wound and hollow fiber tubes. Hollow fiber modules are a common product due to its high surface area to volume ratio which provides the ability to achieve a given separation while occupying a much smaller space.

There are two types of membrane material available; Organic membrane and inorganic membrane. Examples of inorganic are such as carbon or ceramic based material. Ceramic membranes have the advantage of water resistant, thermally stable, chemically resistant and good wear properties [2]. Example of such ceramics are as; γ-alumina, zirconia, titania and silica [3]. In an effort to find alternative cheaper ceramic membrane, Kaolin has been explored as an alternative material for hollow fiber membrane [4].

Spinning technique used in fabrication of hollow fiber membrane is a complex process and encompasses various spinning variables. The membrane morphology, mechanical properties and performance are governed by spinning conditions such as the shear rate; bore fluid rate air gap, spinneret design, material properties and other factors [5, 6, 7, 8, 9].

In a spinning process, a viscous polymer solution is extruded through the small size annulus of a spinneret. It is subjected to shear stress even though the traversing time of a polymeric dope solution is normally short as it involves only a few millimeters in the annulus. Other researchers have investigated and ascertained that the presence of flow induces shear stress affect the rheological behavior of the suspension [5, 10, 11, 12]. The particles of the fluid move relative to each other so that they have different velocities, causing the original shape of the fluid become distorted [13]. The dope solution itself does not follow typical Newtonian fluid behavior [14] further complicates the flow mechanism inside the spinneret. Therefore, it is vital to study the fluid behavior and its correlation with spun hollow fibers morphology.

Computational fluid dynamics (CFD) technology makes it possible to study the shear rate induced in a straight spinneret. The technologies have been used extensively in prior research to understand and established correlation between fluid flow profiles and hollow fiber performance [15, 16]. However, current study of shear rate and elongation rate are mainly on organic membrane. To the author's knowledge, no study has been reported on the use of CFD method to simulate inorganic dope solution flow profile and establish correlation with the hollow fiber microstructure.

The objective of this paper is to study the effect of shear rates induced in a straight spinneret on Kaolin/PESf hollow fiber morphology. To achieve this objective, the following sub objective were completed as well; (1) Spinneret design; (2) CFD study of shear rate profile; (3) Hollow fiber morphology study of hollow fiber at various extrusion rate and material properties; (4) Correlation of shear rate profile and hollow fiber morphology.

EXPERIMENTS: HOLLOW FIBER SPINNING

Materials

Kaolin powders, polyethersulfone (PESF) in pellet form and N-methyl-2-pyrrolidone (NMP, 99% extra pure) were purchased from Sigma Aldrich; each were used as a binder and solvent. The dope solution were prepared as a procedure published elsewhere [17], whose rheological properties were determined by using Brookfield's Programmable HADV-IV + Rheometer. Two

type of dope solution with different Kaolin ratio were used as shown in Table-1.

Table-1. Dope solution properties.

Properties	S1	S2
Kaolin	27 g	54 g
PESf	27 g	27 g
Consistency factor, K (Pa.s)	1.9953	2.5527
Flow Index (*n*)	0.7	0.8

The suspension obeys the power law model commonly associated with the polymeric fluid behaviour. A power law model is normally presented with Equation 1.

$$\tau = K\dot{\gamma}^n \tag{1}$$

Spinning of hollow fiber membrane

Asymmetric hollow fiber membranes were fabricated through wet spinning process. The synthesized dope solution was transferred into a stainless steel dope reservoir, from which dope was fed into the annulus of the spinneret under pressurized nitrogen gas. The nitrogen and bore fluid was set to desired pressure and flow rate, respectively. A 50-liter coagulation bath was initially prepared prior of the spinning process. The bore fluid was let to flow prior the dope extrusion, and then gas control valve was opened slowly to control the dope flow. Tap water at 25 ^{0}C was used as the external coagulant agent in the coagulation bath. The spun fibers were rinsed with water at room temperature for at least 24 hour to remove the residue NMP. The process is then repeated for each different nozzle length and the coagulant (water) was renewed for each spinning process. Detail spinning condition is shown in Table-2.

Morphology study

The hollow fiber morphology was observed under Scanning Electron Microscope (SEM). The preparation procedures are as follow; the fibers are first dried to ensure liquid are removed from the specimen. Then, it is quenched in a liquid nitrogen solution, which brought the specimen to cryogenic state. Next, a thin layer of Joel JFC-11-E is sputtered on the fiber membrane using a sputting device. Finally, images of the hollow fiber membrane were taken at various magnification size.

Table-2. Dope solution properties.

Spinning parameter	Condition
Dope Extrusion Rate (Bar)	0.3,0.4,0.5
Dope/Bore Flow rate Ratio	0.5
Bore fluid	Tap water
Spinning temperature (^{0}C)	28
Humidity (%)	60
Take-up speed	Free fall
Spinneret Dimension (mm)	ID/OD 1.6/3
Spinneret Conv. Angle (^{o})	90 (straight)

CFD SIMULATIONS

Problem statement

To understand the shear rate flow field at various extrusion rate, Solidworks Floworks software package was used. The design geometry of the straight annulus spinneret used to spin the hollow fiber membrane is shown in Figure-1. To simplify the simulation work while not sacrificing result accuracy, the following assumptions were made; (1) L/D ratio greater then 10 to provide fully developed flow (2) Simulation covers only in the annulus (3) 2-Dimensional axisymmetric simulation (4) Steady state condition (5) Homogeneous suspension (6) Atmospheric pressure at outlet (7) No slip boundary condition.
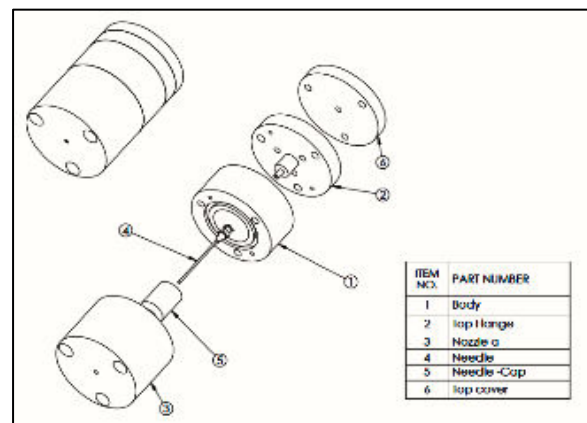

ITEM NO.	PART NUMBER
1	Body
2	Top Flange
3	Nozzle a
4	Needle
5	Needle -Cap
6	Top cover

Figure-1. Spinneret assembly.

Governing equations

Computational fluid dynamics uses numerical techniques to solve fluid flow equations and demonstrate them in much more presentable manner. Solidworks flow simulation solve the Navier-Stokes equation which involve the conservation law for mass, angular momentum and energy which are presented in the Cartesian coordinate system can be written as follow [18]:

$$\frac{\partial \rho}{\partial t} + \frac{\partial}{\partial x_i} = 0 \tag{2}$$

$$\frac{\partial \rho u_i}{\partial t} + \frac{\partial}{\partial x_j}(\rho u_i u_j) + \frac{\partial \rho}{\partial x_i} = \frac{\partial}{\partial x_j}(\tau_{ij} + \tau_{ij}^R) + S_i \qquad (3)$$

$$\frac{\partial \rho H}{\partial t} + \frac{\partial \rho u_i H}{\partial x_i} = \frac{\partial}{\partial x_i}(u_j(\tau_{ij} + \tau_{ij}^R))$$
$$+ \frac{\partial \rho}{\partial t} - \tau_{ij}^R \frac{\partial u_i}{\partial x_j} + \rho\varepsilon + S_i u_i + Q_H \qquad (4)$$

The working fluid in this study exhibit a Non-newtonian power law behavior as found by Suffian *et al*., 2014. The power law model described as follows [18]:

$$\mu(\dot{\gamma}) = K.(\dot{\gamma})^{n-1} + \frac{\tau_o}{\dot{\gamma}} \qquad (5)$$

Where $n > 1$, $\tau_O = 0$ describes the power law model of shear-thickeningnon-Newtonian liquids.

Grid independence study

A grid independence test was done to ensure that a good balance of solution quality and processing resources achieved. Computational meshes for the geometries were generated using Solidworks Floworks system predefined and then customized for better accuracy. For this simulation, a combination of hexahedral and tetrahedral elements was used. Table-3 shows mesh statistics for coarse and fine quality meshes.

Table-3. Mesh statistics.

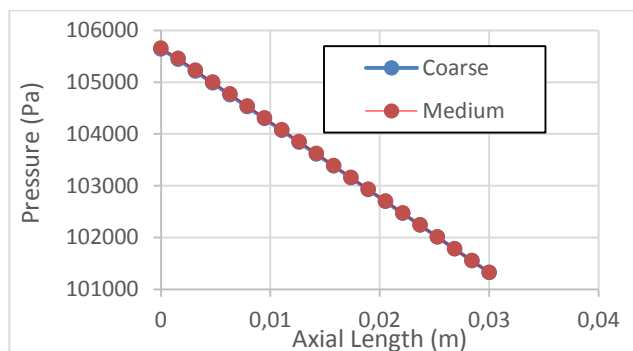| Geometry	Quality	Cell Type	No. of Elements
Straight	Coarse	Fluid	16768
		Solid	3812
		Partial	4872
Straight	Fine	Fluid	36912
		Solid	4550
		Partial	6824

Figure-2. Pressure profile along axial axis for straight spinneret (dope extrusion pressure; 0.3 bar).

Pressure profiles along the axial axis for straight construction are shown in Figure-2. The profile shows the pressure drops to atmospheric pressure as it approach the exit of the spinneret. The profiles were generated in coarse and medium meshes and it shows excellent agreement of each other. The largest deviation observed was at 0.02 % at the early portion of the annulus. Given the time required to reach convergence were relatively quick (5 minutes) for medium mesh, it was used for the rest of the simulation work.

RESULT AND DISCUSSIONS

Shear rate profile of dope solution by CFD simulation

Figure-3 shows a quantitative value of the axial velocity at the outlet of the straight spinneret for both Kaolin/PESf ratio 1 and 2 (S1 and S2). The axial velocity of dope solution peak at the center of the tube typical of a simple pipe flow behavior. The shear rate of the dope solution at the outlet of the straight spinneret are as shown in Figure-4. The shear rate were maximum value near the wall of the spinneret and exhibits minimum value at the center of the convex. There are no clear deviation between Kaolin/PESf ratio in terms of dope solution axial velocity and shear rate. Table-4 show axial velocity and shear rates statistics at outermost point of the tube.

Hollow fiber morphology

Figure-5 shows the SEM imaging study of the cross section at different extrusion rate and material properties, respectively. Generally, the fiber precursors demonstrated an asymmetrical structure. It consists of sponge like structure and finger like void structure coming from the inner and outer surfaces. Similar observation were noted by past study, which states that fibre morphologies for a ceramic/polymer system are comprise of finger-like voids and sponge-like structures.

It can be seen from Figure-5 and 6 that the inner and outer surface of these hollow fiber to be porous. The mechanism of interconnected open cell structure are interrelated to those of organic membrane and thus stated here with; liquid-liquid demixing process took place either in the outer or inner fiber precursor surface. Leading to nucleation or growth of the localized polymer rich phase that produce polymer agglomerates. Generally, an inner surface have a higher porosity due to delayed liquid-liquid demixing due high solvent concentration in the bore fluid. Higher density is observed at the outer skin due to instantaneous liquid-liquid demixing process. Where as, the sponge like structure in the center of the fibre was attributed to a slow precipitation. With the increases of the extrusion rate, possibly the outer skin of the hollow fiber membrane become denser. This is due to the molecular chain tends to align themselves better and form a compact structure together, leading to a denser structure [11].

Figures 7 and 8 shows inner and outer structure of hollow fiber membrane at two different material properties; S1 with lower viscosity and S2 with a higher density. The image shows that at lower viscosity the outer finger like structures dominates the fibre cross sections while at higher viscosity, inner finger like structure dominates. The trend continues at different extrusion rates as well.
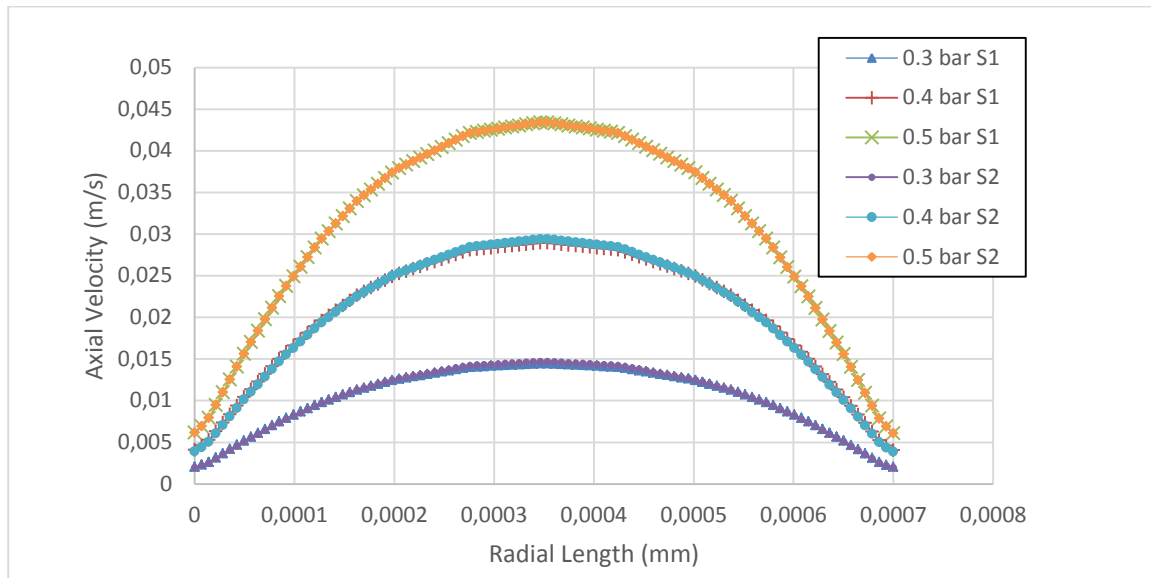
www.arpnjournals.com

Figure-3. Axial velocity at spinneret outlet.
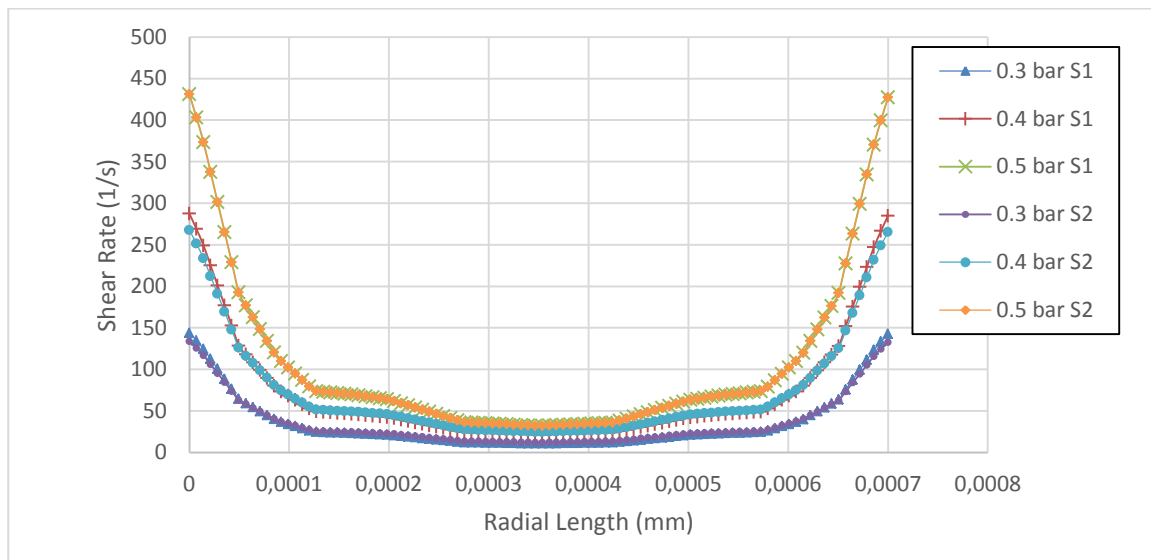

Figure-4. Shear rate at spinneret outlet.

Table-4. Axial velocity and shear rate statistics for straight spinnerets.

Dope extrusion pressure (bar)	Max. axial velocity (m/s)		Max. shear rate (1/s)	
	S1	**S2**	**S1**	**S2**
0.3	0.01446	0.01469	143.78	133.81
0.4	0.02885	0.02938	287.48	267.59
0.5	0.04341	0.04341	431.03	431.03

www.arpnjournals.com

a. Extrusion pressure: 0.3 bar(S1)

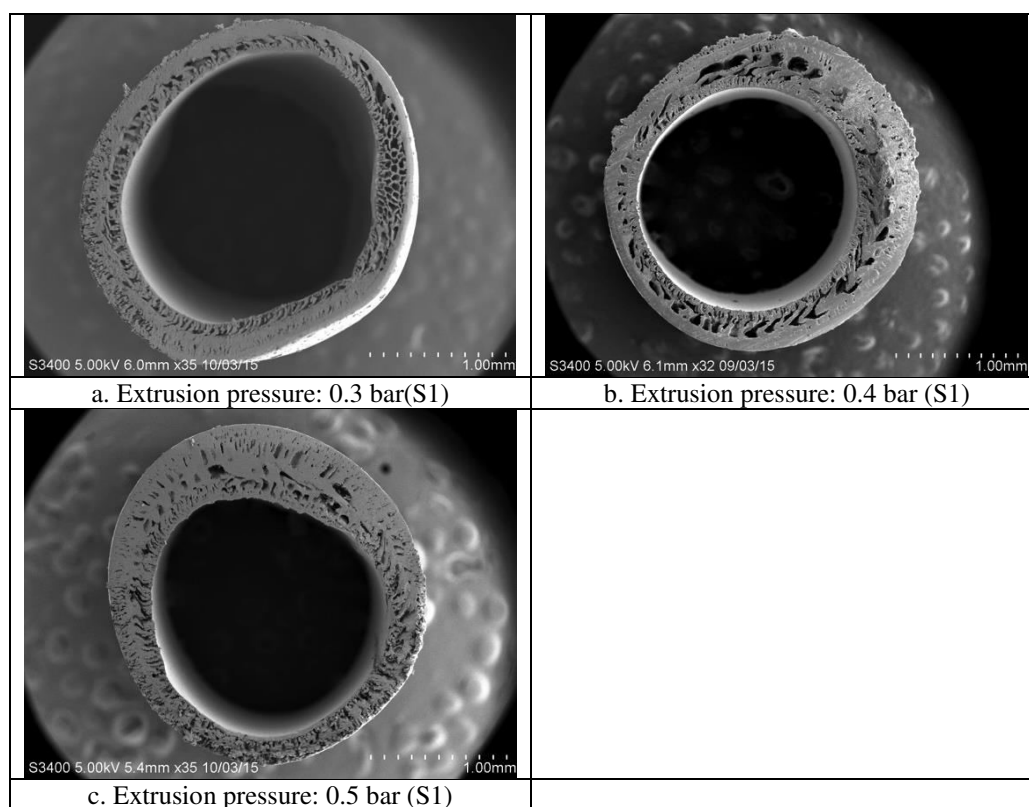b. Extrusion pressure: 0.4 bar (S1)

c. Extrusion pressure: 0.5 bar (S1)

Figure-5. Cross section of hollow fiber for sample S1 (a, b, and c for extrusion pressure of 0.3, 0.4, and 0.5 bar respectively).

a. Extrusion bar: 0.3bar (S2)
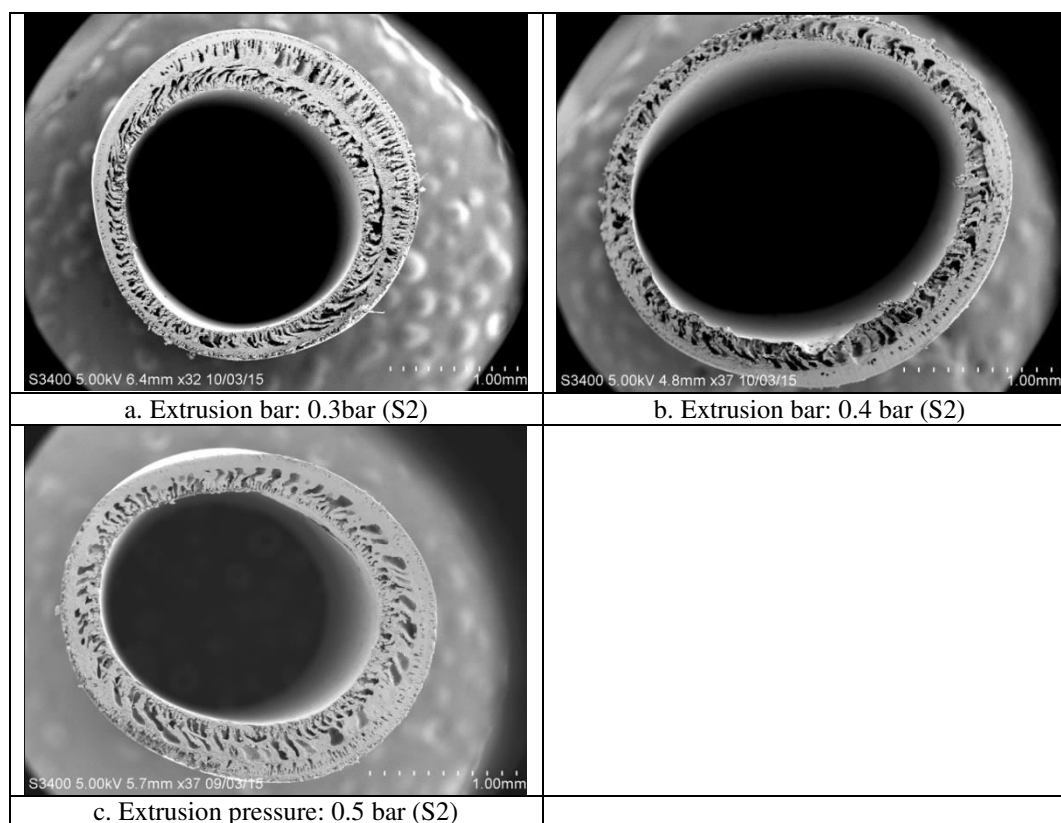
b. Extrusion bar: 0.4 bar (S2)

c. Extrusion pressure: 0.5 bar (S2)

Figure-6. Cross section of hollow fiber for sample S2 (a, b, and c for extrusion rate of 0.3, 0.4, and 0.5 bar respectively).

a. Extrusion pressure: 0.3 bar (S1)

b. Extrusion pressure: 0.4 bar (S1)
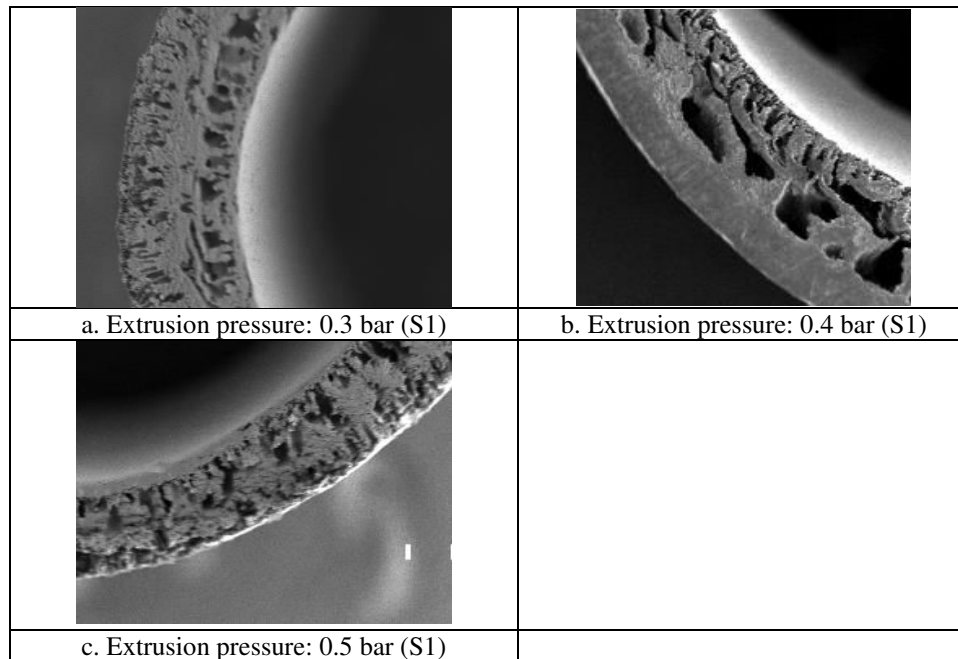
c. Extrusion pressure: 0.5 bar (S1)

Figure-7. Inner/outer edge cross section of hollow fiber for sample S1 (a, b, and c for extrusion pressure of 0.3, 0.4, and 0.5 bar respectively).

a. Extrusion pressure: 0.3 bar (S2)

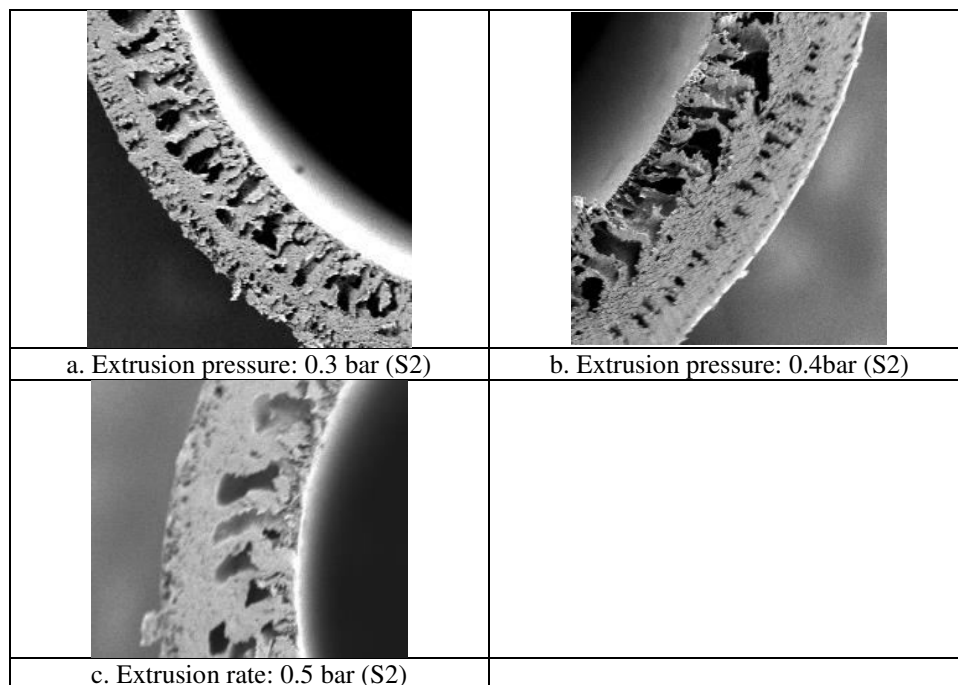b. Extrusion pressure: 0.4bar (S2)

c. Extrusion rate: 0.5 bar (S2)

Figure-8. Inner/outer edge cross section of hollow fiber for sample S2 (a, b, and c for extrusion pressure of 0.3, 0.4 and 0.5 bar respectively).

CONCLUSIONS

This paper has successfully presented the effect of shear rate to the morphology of Kaolin/PESf hollow fiber membrane precursor by using a straight spinneret at various extrusion rate and material properties. CFD technologies have been successfully implemented to analyze the shear rate flow field at the exit of the annulus and gave us a better picture of shear stress distribution in that area. Ultimately, shear stress effect the morphology of the hollow fiber membrane where existing hypothetic mechanism were utilize to explain the phenomena. Such finding is important as extrusion rate is one of the spinning variables that can be a factor to get a desired hollow fiber precursor property. The study also confirm that based on existing hypothetic mechanism mention in previous study [5], shear rate primarily align polymer chain forming a denser voids which in turn might contribute to better permeance characteristic.

In future work, the researcher should tackle the effect of elongation rate on hollow fiber morphology. Elongation rate only occurs in conical spinneret and does not exist in a straight spinneret. Additionally, improvement need to be taken to address the quality of the hollow fiber membrane as current sample shows defects and inconsistent quality of the fiber precursor.

REFERENCES

[1] Loeb S., Sourirajan S. 1963. Sea water demineralization by means of osmotic membrane. 117-132.

[2] Van Rijn. 2004. Nano and micro engineered membrane technology. Elsevier.

[3] deFriend K.A., Wiesner M.R., and A.R. Barron. 2003. Alumina and aluminate ultra-filtration membranes derived from alumina nanoparticles. Journal of Membrane Science. 224:11–28.

[4] Sarbatly R. and Kamin Z. 2013. The effects of Kaolin/PESF Ratios on the microstructures of kaolin hollow tubes. In: R. Pogaku, Developments in Sustainable Chemical 381 and Bioprocess Technology, Springer Science+Business Media, New York. 381-387.

[5] Chung T. S., Qin J. J., and Gu J. 2001. Effect of shear rate within the spinneret on morphology, separation performance and mechanical properties of ultrafiltration polyethersulfone hollow fiber membranes. Chemical Engineering Science. 56: 5869.

[6] Porter M. C. 1990. Handbook of Industrial Membrane Technology. New Jersey, USA: Noyes.

[7] Niwa M., Kawakami H., Nagaoka S., Kanamori T., and Shinbbo T. 2000. Fabrication of an asymmetric polyimide hollow fiber with a defect-free surface skin layer. Journal of Membrane Science. 171(2): 253-261.

[8] Piau J. M., Kissi N. E., and Tremblay B. 1988. Low Reynolds number flow visualization of linear and branched silicones upstream of orifice dies. Journal of Non-Newtonian Fluid Mechanics. 30:197

[9] Yang Q., Chung T. S., Chen S. B., and Weber M. 2008. Pioneering explorations of rooting causes for morphology and performance differences in hollow fiber kidney dialysis membranes spun from linear and hyperbranched polyethersulfone. Journal of Membrane Science. 313: 190.

[10] Wang K. Y., Matsuura T., Chung T. S., and Guo W. F. 2004. The effects of flow angle and shear rate within the spinneret on the separation performance of poly (ethersulfone) (PES) ultrafiltration hollow fiber membranes. Journal of Membrane Science.240: 67.

[11] Qin J. J., Gu J. and Chung T. S. 2001. Effect of wet and wet-jet spinning on the shear-induced orientation during the formation of ultrafiltration hollow fiber membranes. Journal of Membrane Science.

[12] Chung T. S., Teoh S. K., Lau W. W. Y., and Srinivasan M. P. 1998. Effect of shear stress within the spinneret on hollow fiber membrane morphology and separation performance. Industrial and Engineering Chemistry Research. 37: 3930.

[13] John F. D., Janusz M. G., and John A. S. 2001. Fluid mechanics. Essex, England: Pearson Education Limited.

[14] Bird R. B., Armstrong R. C., and Hassager O. 1987. Dynamics of polymeric liquids fluid mechanics. Vol. 1, 2nd Ed., John Wiley and Sons.

[15] Kuo-Lun T., Yu-Ling L., Che-Chia H., and Yu-Shao C. 2012. Power-Law polymer solution flow in a converging annular spinneret: Analytical approximation and numerical computation. American Institute of Chemical Engineers AIChE Journal. 58: 122–131.

[16] Widjojo N., Chung T. S., Arifin D. Y., Weber M., and Warzelhan V. 2010. Elimination of die swell and instability in hollow fiber spinning process of hyperbranched polyethersulfone (HPES) via novel spinneret designs and precise spinning conditions. Chemical Engineering Journal. 163: 143-153.

[17] Suffian M., Rosalam S., and Mizanur R. 2014. Rheological properties of kaolin/polyethersulfone (PESf) used in hollow fiber fabrication: Effects of content ratio. Applied Mechanics and Materials.

[18] Solidworks Flow Simulation. 2012. Technical Reference, Solidworks Inc.